PERGAMON

International Journal of Heat and Mass Transfer 42 (1999) 723–737

International Journal of HEAT and MASS TRANSFER

Comparison of low Reynolds number k–ε models in simulation of momentum and heat transport under high free stream turbulence

Ganesh R. Iyer*, Savash Yavuzkurt

Department of Mechanical Engineering, Center for Gas Turbines and Power, The Pennsylvania State University, University Park, PA 16802, U.S.A.

Received 29 July 1997; in final form 4 June 1998

Abstract

Calculations of the effects of high free stream turbulence (FST) on the transport of momentum and heat in a flat plate turbulent boundary layer are presented. Four well known low Reynolds number k–ε models namely Launder–Sharma, K.-Y. Chien, Lam–Bremhorst and Jones–Launder were used in order to investigate specifically their prediction capabilities under high FST conditions (initial FST intensity, $Tu_i > 5\%$). These models were implemented in computer code TEXSTAN, a partial differential equation solver which solves steady flow boundary layer equations. Firstly, these models were compared with empirical data and standard correlations to test how they predicted very low FST ($Tu_i = 1\%$) cases. Predictions of all models for skin friction and heat transfer were good (within $\pm 5\%$ of data and correlations) with the exception of the Lam–Bremhorst model which predicts skin friction and heat transfer within about 10% of empirical data and correlations. For turbulent kinetic energy (TKE) profiles, Jones–Launder and Launder–Sharma models had problems predicting the peak value of TKE. Subsequently, all these models were used in order to predict the effects of high FST ($Tu_i > 5\%$). Predictions became poorer (over-prediction up to more than 50% for skin friction and Stanton number, and under-prediction of TKE up to more than 50%) as FST increased to about 26%. The high FST data sets against which the predictions were compared had initial FST intensities of 6.53% and 25.7%. Physical reasoning as to why the aforementioned models break down with increasing FST is given.

Nomenclature

c_f skin friction coefficient
c_σ skin friction coefficient at low FST
c_μ, c_1, c_2 constants in two-equation turbulence models
f_1, f_2, f_μ low Reynolds number functions
FST free stream turbulence
h mean static enthalpy [J kg^{-1}]
h' fluctuating static enthalpy [J kg^{-1}]
k TKE (turbulent kinetic energy) [m^2 s^{-2}]
k_∞ TKE in the free stream [m^2 s^{-2}]
L^u_∞ streamwise turbulence dissipation length scale in the free stream [m]
P static pressure [Pa]
Pe_t turbulent Peclet number
Pr Prandtl number
Pr_t turbulent Prandtl number
Re_θ Reynolds number based on momentum thickness
Re_x Reynolds number based on length of heating along the flat plate
Re_T turbulent Reynolds number
St Stanton number
T_w wall temperature [K]
T_∞ free stream temperature [K]
Tu free stream turbulence intensity, %
Tu_i initial (at the start of calculations) free stream turbulence intensity, %
u'^2, v'^2, w'^2 normal Reynolds stresses in x, y and z directions [m^2 s^{-2}]
u^* friction velocity [m s^{-1}]

* Corresponding author: Automated Analysis Corporation, 423 S.W. Washington, Peoria, IL 61602, U.S.A.

0017–9310/98 $19.00
PII: S0017–9310(98)00194–X

u^+, y^+ inner variables
U mean veloity in the x direction (direction of flow) [m s^{-1}]
U_∞, U_f free stream velocity in the x direction (direction of flow) [m s^{-1}]
V mean velocity in the y direction [m s^{-1}]
x streamwise coordinate (in the direction of flow) [m]
y coordinate normal to the direction of flow [m].

Greek symbols
δ momentum boundary layer thickness [m]
δ^* displacement thickness [m]
$\tilde{\varepsilon}$ modified turbulent dissipation rate variable [m^2 s^{-3}]
$\tilde{\varepsilon}_\infty$ free stream turbulent dissipation rate [m^2 s^{-3}]
ε_f initial free stream Turbulent dissipation rate [m^2 s^{-3}]
κ von-Karman constant
μ dynamic viscosity [Pa s^{-1}]
μ_t eddy viscosity [Pa s^{-1}]
ν kinematic viscosity [m^2 s^{-1}]
θ momentum thickness [m]
ρ density [kg m^{-3}]
σ_k, σ_ε constants in two-equation turbulence models
τ_w wall shear stress [N m^{-2}].

Subscripts
∞, f free stream conditions
t turbulent
w wall
0 low FST condition.

1. Introduction

Free stream turbulence (FST) is turbulence in the approach stream. It is well known that FST influences turbulent boundary layers. Examples of high FST environments include nozzle guide vanes, gas turbine blades and heat exchanger flows, where it is very important to predict both boundary layer development and convective heat transfer coefficients. Gas turbine engines run with turbulence intensities greater than 20% [1] and the turbulence in the free stream is highly anisotropic and consist of large eddies generated from the combustion chamber or wakes of blades. High FST environments are known to enhance surface heat transfer and its is very important that these enhanced values be known for design purposes.

Free stream turbulence intensity, Tu, which is going to be often used through out this document is defined as follows:

$$Tu = \left(\frac{\sqrt{\overline{u'^2} + \overline{v'^2} + \overline{w'^2}/3}}{U} \right)_\infty \tag{1}$$

In some experimental investigations, $\overline{v'^2}$ and $\overline{w'^2}$ are not available, and isotropy is assumed leading to the following definition of Tu:

$$Tu = \left(\frac{\sqrt{\overline{\overline{u'^2}}}}{U} \right)_\infty \tag{2}$$

Unless stated otherwise, all the works cited have used equation (2).

A number of empirical studies have been carried out to analyze the effects of FST on a boundary layer. Results of measurements carried out at high Reynolds numbers ($Re_\theta = 6500$) by Simonich and Bradshaw [2] showed that grid generated FST increased the heat transfer by about 5% for each 1% rms increase of the longitudinal intensity. The data of Pedisius et al. [3] was the first to suggest without a doubt, a marked increase in Stanton number (up to 40%) under high FST conditions (up to initial turbulence intensity of 24%). Both, Simonich and Bradshaw [2] and Pedisius et al. [3] correlated increases in Stanton number with Tu alone. For a long time, the responses to variations in the ratio of FST length scale to the boundary layer thickness was underestimated. Hancock and Bradshaw [4] apparently showed for the first time that FST length scale was also an important parameter. Their results indicated the decrease of FST effect with increasing length scale ratio at least in the range $0.7 < L^u_\infty/\delta < 5.5$, where L^u_∞ is the streamwise turbulence dissipation length scale defined by the following equation,

$$U_\infty \frac{\mathrm{d}(\overline{u'^2_\infty})}{\mathrm{d}x} = \frac{-(\overline{u'^2_\infty})^{3/2}}{L^u_\infty} \tag{3}$$

They found an empirical correlation that relates the increase in skin friction coefficient at constant Re_θ to a FST parameter β which accounts for effects of both the turbulence intensity and length scale:

$$\frac{\Delta c_f}{c_{f_0}} = f(\beta) \quad \text{where} \quad \beta = \frac{100Tu}{\frac{L^u_\infty}{\delta} + 2} \tag{4}$$

Δc_f in the above equation is the change in skin friction coefficient c_f from the low FST value (c_{f0}) at the same Re_θ. Apart from the work of Hancock and Bradshaw [4], a number of researchers have carried out important experimental work concerning effects of FST (intensity and length scale) on a boundary layer and some of these can be found in [5–11].

In the area of modelling, Harasgama et al. [12] employed several k–ε models for the calculation of heat transfer to turbine blades. It was concluded that the modified Lam and Bremhorst Production Term Modification (LBPTM) formulated by Schmidt and Patankar [13] was successful in predicting accurately all the cases on the pressure side (in terms of heat transfer coefficient). Results also showed that the suction side of the blade was more difficult to predict and suggested that the models if used appropriately will yield good predictions of turbine blade heat transfer. The maximum turbulence intensity

and Mach number for the test cases were 6% and 1.089 respectively. They pointed out the need for better models that could be applied to high Mach number cases. Sieger et al. [14] compared several k–ε turbulence models to predict transition under influence of FST (up to $Tu = 11\%$) and pressure gradient. The test cases included those of Blair and Werle [6, 15], Rud and Wittig [16] and the aerodynamic measurements of Rolls–Royce [17]. They also found that LBPTM model performed the best in matching experimental data in zero as well as non-zero pressure gradient flows at different FST intensities. Models which have the inner variable y^+ in their low Reynolds number functions were not found suitable for predicting transition. For higher Tu, they fail completely in reproducing the laminar and transition regions. Kwon and Ames [18] formulated a k–ε based velocity and length scale closure model which accounts for the anisotropy of the dissipation and the reduced length of mixing due to the high strain rates present in the near wall region. This work was definitely a step towards advancing k–ε modelling to predict high FST flows. In this model, the velocity scale v' in the eddy viscosity formulation ($\mu_t = \rho v' l$) was evaluated by integrating the normal component energy spectrum. The length scale was obtained from the local distance from the wall. The energy spectrum was based on the local dissipation rate; k and ε were obtained from the corresponding transport equations of Durbin [19]. Heat transfer predictions obtained from this model compared well with the experimental data ($Tu = 19\%$) of Ames and Moffat [7]. Fridman [20] implemented an algebraic relaxation-length model of turbulence to predict the influence of high FST on heat transfer coefficients for a flat plate turbulent boundary layer with zero pressure gradient and in the vicinity of the stagnation point of a circular cylinder. The calculation results for heat transfer and skin friction coefficients, for velocity and temperature profiles, for Reynolds stresses and turbulent heat fluxes are in fair agreement for turbulent boundary layers. Very recently, Volino [21] developed a model which incorporated a free stream induced viscosity besides the eddy viscosity μ_t and molecular viscosity μ. This viscosity is modeled with the aid of empirical data and scales on the fluctuating rms normal velocity in the free stream (obtained from experiments and assumed constant in the streamwise direction), the distance from the wall and δ, the boundary layer thickness. This new model was used in combination with a mixing length model to obtain good predictions for Tu ranging from 1 to 8% and for both zero and non-zero pressure gradient cases. Other important simulation work for predicting effects of FST on a boundary layer can be found in refs [22] and [23].

2. Objectives

Although a plethora of experimental work has been done in the area of FST, comparatively lesser efforts have been made in the modelling domain for predicting effects of FST on a turbulent boundary layer. In fact, very few attempts have been made to compare the existing two-equation models for external turbulent flow under high FST ($Tu_i > 5\%$) conditions. More importantly, research done in turbulence modelling community hitherto have focused on predicting heat transfer and skin friction coefficients but not much on TKE. Admittedly, current models [18, 20, 21] predict heat transfer coefficient well for some cases, but the significance of correct prediction of TKE is not emphasized. While agreeing with the fact that it is very important to rightly predict skin friction and heat transfer coefficients, arguably, good prediction of TKE is also equally important. In fact, correct prediction of TKE should ensure good predictions of skin friction and heat transfer coefficients since TKE is used to calculate the turbulent transport coefficient μ_t. With this in mind, it was decided to realize the following objectives:

(1) To test and compare the prediction capabilities of four k–ε models namely, Jones and Lauder (JL) [24], Launder and Sharma (LS) [25], Lam and Bremhorst (LB) [26] and Chien (KYC) [27] for predicting skin friction coefficient, heat transfer and TKE under high FST ($Tu_i > 5\%$) conditions. These four models were chosen, primarily because they are among the well tested models. It is hoped that such a comparison of the models under high FST conditions would eventually lead to development of better and physically sound models for predicting very important applications like gas turbine and heat exchanger flows. The computer program TEXSTAN [28] which contained these models was used for all the predictions.
(2) To give plausible physical reasoning for the behavior of these models under high FST conditions.

3. Computer code

The computer code TEXSTAN is a partial differential equation solver for a system of parabolic equations. It is based on the original ideas of Patankar and Spalding [29] and solves steady flow boundary layer equations that govern two-dimensional boundary layer flows and channel flows. This program solves x-momentum, energy, mass transfer and turbulent transport (k, ε) equations. The code requires initial profiles and boundary conditions at two bounding surfaces. Patankar's finite volume scheme is implemented for finite differencing with the resultant difference equations linearized.

3.1. Boundary layer equations

For a steady, two-dimensional, incompressible and turbulent flow, the velocity and temperature fields within

the boundary layer are governed by the continuity, momentum and enthalpy equations which are as follows:
Continuity:

$$\frac{\partial U}{\partial x}+\frac{\partial V}{\partial y}=0 \tag{5}$$

x-Momentum:

$$\rho U\frac{\partial U}{\partial x}+\rho V\frac{\partial U}{\partial y}=\frac{\partial}{\partial y}\left[\mu\frac{\partial U}{\partial y}-\rho\overline{u'v'}\right]-\frac{\mathrm{d}P}{\mathrm{d}x} \tag{6}$$

Enthalpy:

$$\rho U\frac{\partial h}{\partial x}+\rho V\frac{\partial h}{\partial y}=\frac{\partial}{\partial y}\left[\left(\frac{\mu}{Pr}\right)\frac{\partial h}{\partial y}-\rho\overline{h'v'}\right]+\frac{\partial}{\partial y}\left\{U\left[\left(1-\frac{1}{Pr}\right)\mu\frac{\partial U}{\partial y}-\rho\overline{u'v'}\right]\right\} \tag{7}$$

In deriving the equations, conventional time averaging was employed. By specifying the appropriate initial and boundary conditions, and a turbulence model for $\overline{u'v'}$ and $\overline{h'v'}$, these equations can be solved.

3.2. Low Reynolds number k–ε models

The k–ε model employs the eddy viscosity concept which relates the Reynolds stress to the mean velocity gradient [24].

$$-\rho\overline{u'v'}=\mu_{\mathrm{t}}\frac{\partial U}{\partial y} \tag{8}$$

The eddy viscosity μ_{t} is determined from the local values of k and $\tilde{\varepsilon}$ [13]:

$$\mu_t=\frac{c_\mu f_\mu \rho k^2}{\tilde{\varepsilon}} \quad \text{and} \quad \varepsilon=\tilde{\varepsilon}+D \tag{9}$$

The quantity D is the value of ε at $y=0$ and is defined for each model. For models where $D=0$, $\tilde{\varepsilon}$ is the same as ε. The local values of k and $\tilde{\varepsilon}$ are calculated from the following time-averaged semi-empirical transport equations [13]:

$$pU\frac{\partial k}{\partial x}+\rho V\frac{\partial k}{\partial y}=\frac{\partial}{\partial y}\left[\left(\mu+\frac{\mu_{\mathrm{t}}}{\sigma_k}\right)\frac{\partial k}{\partial y}\right]+\mu_{\mathrm{t}}\left(\frac{\partial U}{\partial y}\right)^2-\rho\varepsilon \tag{10}$$

$$\rho U\frac{\partial \tilde{\varepsilon}}{\partial x}+\rho V\frac{\partial \tilde{\varepsilon}}{\partial y}=\frac{\partial}{\partial y}\left[\left(\mu+\frac{\mu_{\mathrm{t}}}{\sigma_\varepsilon}\right)\frac{\partial \tilde{\varepsilon}}{\partial y}\right]+\left[c_1 f_1\mu_{\mathrm{t}}\left(\frac{\partial U}{\partial y}\right)^2-\rho c_2 f_2\tilde{\varepsilon}\right]\frac{\tilde{\varepsilon}}{k}+E \tag{11}$$

The term $-\rho\overline{h'v'}$ in the equation (7) is modeled as follows:

$$-\rho\overline{h'v'}=\frac{\mu_{\mathrm{t}}}{Pr_{\mathrm{t}}}\frac{\partial h}{\partial y} \tag{12}$$

The constants c_μ, σ_{k}, and σ_ε are model independent and are equal to 0.09, 1.0 and 1.3 respectively. Pr_{t} is the turbulent Prandtl number and is equal to 0.85 or is determined from the following equation [30]:

$$Pr_{\mathrm{t}}=\frac{1}{\frac{1}{2Pr_{\mathrm{t}\infty}}+CPe_{\mathrm{t}}\sqrt{\frac{1}{Pr_{\mathrm{t}\infty}}}-(CPe_{\mathrm{t}})^2\times\left[1-\exp\left(-\frac{1}{CPe_{\mathrm{t}}\sqrt{Pr_{\mathrm{t}\infty}}}\right)\right]} \tag{13}$$

Pe_{t} is the turbulent Peclet given by

$$Pe_{\mathrm{t}}=\frac{\nu_{\mathrm{t}}}{\nu}Pr. \tag{14}$$

$Pr_{\mathrm{t}\infty}$ is value of Pr_{t} far away from the wall, and is an experimental constant ($=0.85$). C is also another experimental constant and is equal to 0.2. The low Reynolds number functions f_1, f_2 and f_μ, the constants c_1, c_2 and σ_{k}, and the terms D and E are summarized for the different models as follows:

JL model [24]

$$f_\mu=\exp\left(\frac{-2.5}{1+Re_{\mathrm{T}}/50}\right),\quad f_1=1.0,$$

$$f_2=1-0.3\exp(-Re_T^2)$$

where $Re_{\mathrm{T}}=\dfrac{k^2}{\nu\tilde{\varepsilon}}$, $\quad c_1=1.55,$

$$c_2=2.00,\quad D=2\mu\left(\frac{\partial k^{0.5}}{\partial y}\right)^2$$

and $E=2\nu\mu_{\mathrm{t}}\left(\dfrac{\partial^2 U}{\partial y^2}\right)^2$.

LS model [25]

$$f_\mu=\exp\left(\frac{-3.4}{(1+Re_{\mathrm{T}}/50)^2}\right),\quad f_1=1.0,$$

$$f_2=1-0.3\exp(-Re_{\mathrm{T}}^2)$$

where $Re_{\mathrm{T}}=\dfrac{k^2}{\nu\tilde{\varepsilon}}$, $\quad c_1=1.44,$

$$c_2=1.92,\quad D=2\mu\left(\frac{\partial k^{0.5}}{\partial y}\right)^2$$

and $E=2\nu\mu_{\mathrm{t}}\left(\dfrac{\partial^2 U}{\partial y^2}\right)^2$.

KYC model [26]

$$f_\mu=1-\exp(-0.0115y^+),\quad f_1=1.0,$$

$$f_2=1-0.22\exp\left[-\left(\frac{Re_{\mathrm{T}}}{6}\right)^2\right]$$

where $\quad Re_{\mathrm{T}}=\dfrac{k^2}{\nu\tilde{\varepsilon}}$, $\quad c_1=1.35,$

$$c_2 = 1.80, \quad D = 2\mu\left(\frac{k}{y^2}\right)$$

and $E = -2\mu\frac{\tilde{\varepsilon}}{y^2}\exp(-0.5y^+)$.

Here, $y^+ = yu^*/v$ where the friction velocity is defined by $u^* = \sqrt{\tau_w}/\rho$ (τ_w is the wall shear stress).

LB model [27]

$$f_\mu = \left[1-\exp\left(-0.0163Re_y\right)\right]^2 \cdot \left[1+\frac{20.0}{Re_T}\right]$$

where $Re_T = \frac{k^2}{v\tilde{\varepsilon}}$ and $Re_y = \frac{k^{0.5}y}{v}$

$$f_1 = 1.0+\left(\frac{0.055}{f_\mu}\right)^3, \quad f_2 = 1-\exp(-Re_T^2),$$

$$c_1 = 1.44, \quad c_2 = 1.92, \quad D = 0, \quad \text{and } E = 0.$$

The JL and LS models are essentially similar, except for the slight differences in the values of f_μ, c_1 and c_2. The extra term E in the JL, LS and KYC models was included to adjust the peak value in the TKE profile. The constants f_μ, c_1 and c_2 for the KYC model are slightly different from the JL model, although the difference between the constants c_1 and c_2 is kept the same considering the fact that production and dissipation of TKE are nearly in balance in wall flows. The LB model differs from all these models mainly in that it does not contain any extra terms (D and E) in k and ε equations.

3.3. Initial profiles and boundary conditions

Since profiles of TKE are going to be compared with experimental data in the next section, a discussion of initial profiles and boundary conditions are in order. The initial velocity, temperature, kinetic energy and dissipation rate profiles in the inner and outer region of the turbulent boundary layer, generated by TEXSTAN, were derived from mixing length arguments. This was done in order to have a consistent approach, since all experimental initial profiles are not reported for some of the data sets used.

Regarding boundary conditions, for all the four models and for all the cases to be shown, the velocity $U = 0$ at the flat plate wall and $U = U_\infty$ in the free stream were applied. The free stream temperatures were constant for all cases considered but the wall temperature varied (due to constant heat flux) with x-direction (i.e. direction of flow). For variable wall temperature, the temperature was linearly interpolated between x-locations. For TKE, $k = 0$ at the wall was applied for all the models examined. Except for the LB model, the wall condition $\tilde{\varepsilon} = 0$ was applied for the dissipation rate. For the LB model the boundary condition

$$\frac{\partial\tilde{\varepsilon}}{\partial y} = 0$$

was applied at the wall. The specification of initial values of free stream k_∞ and $\tilde{\varepsilon}_\infty$ was sufficient to integrate the following equations which are the limiting free stream forms of equations (10) and (11).

$$U_\infty\frac{\mathrm{d}k_\infty}{\mathrm{d}x} = -\tilde{\varepsilon}_\infty \tag{15}$$

$$U_\infty\frac{\mathrm{d}\varepsilon_\infty}{\mathrm{d}x} = \frac{-c_2f_2\tilde{\varepsilon}_\infty^2}{k_\infty} \tag{16}$$

Values of c_2 for all the models were mentioned in the previous section and f_2 is unity in the free stream for all the models.

The grid size used to generate the initial profiles for the boundary layer computations are given by the following formula:

$$\Delta y = \Delta y_1(1+\text{rate})^{i-2}; \quad \Delta y \leqslant 0.035y_{\text{edge}} \tag{17}$$

Δy_1 locates the first grid point, i is the cross stream index and y_{edge} is the calculated value of boundary layer thickness. For all the computations the value of rate was 0.09, since it yielded grid independent solutions.

4. Results and discussion

4.1. Model predictions in the turbulent region for very low FST (baseline case)

Baseline ($Tu_i = 1\%$) test cases were run for all the models (constant property calculations) with Pr_t being constant and equal to 0.85. These results were compared with experimental data and empirical correlations. Figure 1a shows the plot of skin friction coefficient versus Reynolds number based on momentum thickness. The figure indicates that the predictions of TEXSTAN match very well for JL, LS and KYC models (within $\pm 5\%$) with the experimental data of Wieghardt–Tillman [2] and also the correlation of Kays and Crawford [30] which is:

$$\frac{c_f}{2} = 0.0125Re_\theta^{-0.25} \tag{18}$$

The LB model also performs reasonably well (within 4–8%) when compared with data and correlation. Heat transfer baseline test is represented by the plot (Fig. 1b) of Stanton number (St) versus Reynolds number based on length of heating. Here, the JL, LS and KYC model predictions compare reasonably well (within about 8%) with data and the correlation of Kays and Crawford [30] which is given below.

$$StPr^{0.4} = 0.03Re_x^{-0.2} \tag{19}$$

The LB model does not perform well relatively (within 14% of data and correlation). Dimensionless TKE profiles at $Re_\theta = 7700$ indicate that all the models match

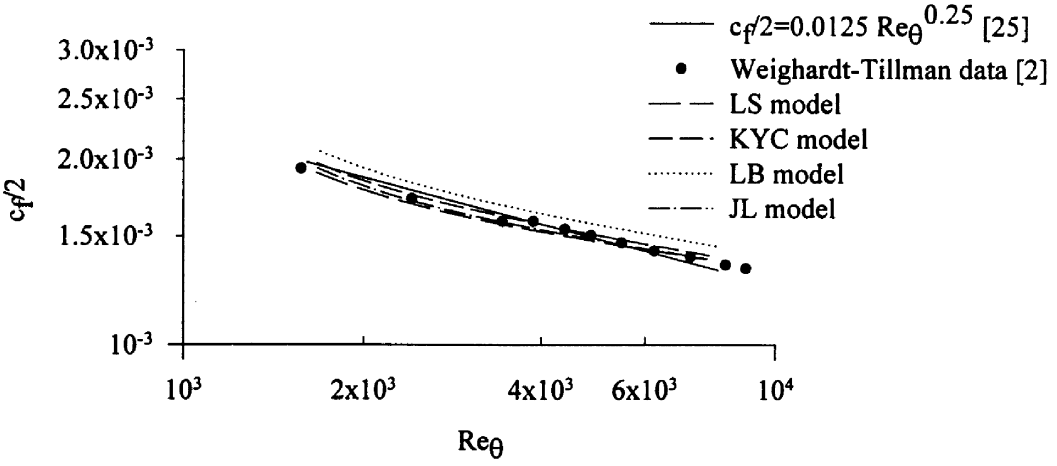

Fig. 1a. Skin friction coefficient for baseline case ($Tu_i = 1\%$).

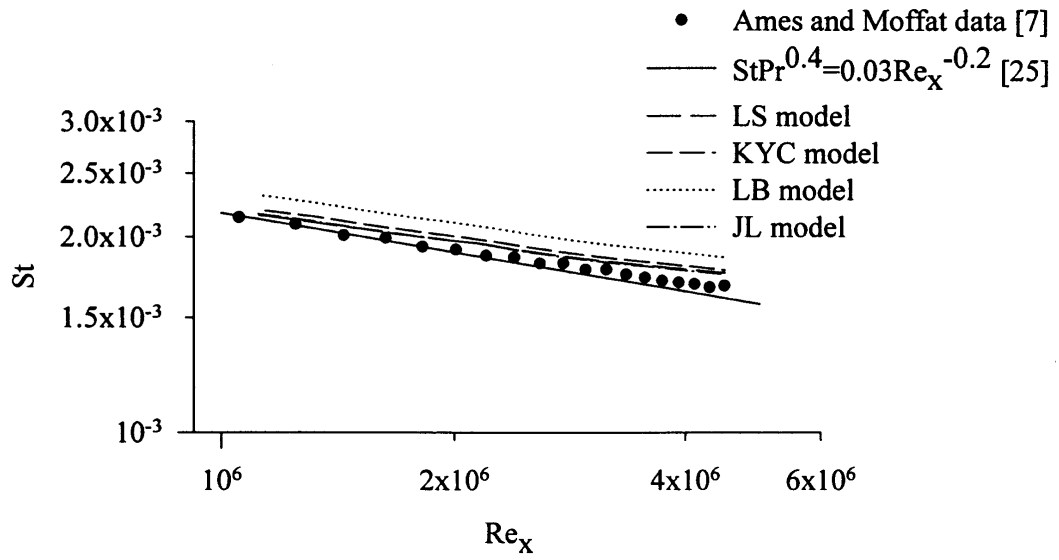

Fig. 1b. Stanton number for baseline case ($Tu_i = 1\%$).

reasonably well with measurements of Klebanoff [26] (within 2–9%) in the region up to y/δ approximately equal to 0.4 (Fig. 1c). Predictions by the JL and LS models though, get worse in the near wall region. They yield peak values (0.0053 and 0.0046) respectively which are considerably lower than the peak in measurements (0.0065). The LB model deviates from the peak by about 10% and the KYC predicts the best (within 3% of experimental data). All models seem to over predict more as one approaches the free stream edge because all the cases were run at Tu_i of 1%, whereas the data is usually taken at much less than 1% ($\leqslant 0.4\%$). Running cases at $Tu_i < 1\%$ lead to numerical instability. Agreement of predictions for velocity profiles (Fig. 1d) of all the models with empirical data is good. The predictions also match well with Spalding's [31] correlation which is given as follows:

$$y^+ = u^+ + e^{-\kappa B}[e^{\kappa u^+} - 1 - \kappa u^+ - (\kappa u^+)^2/2 - (\kappa u^+)^3/6] \tag{20}$$

In the above equation $\kappa = 0.41$ and $B = 5.0$. This correlation is an excellent fit to near wall data all the way from the wall to the point (usually for $y^+ > 100$), where the outer layer profile begins to deviate and rise above the logarithmic curve.

These models were also tested for turbulent Prandtl

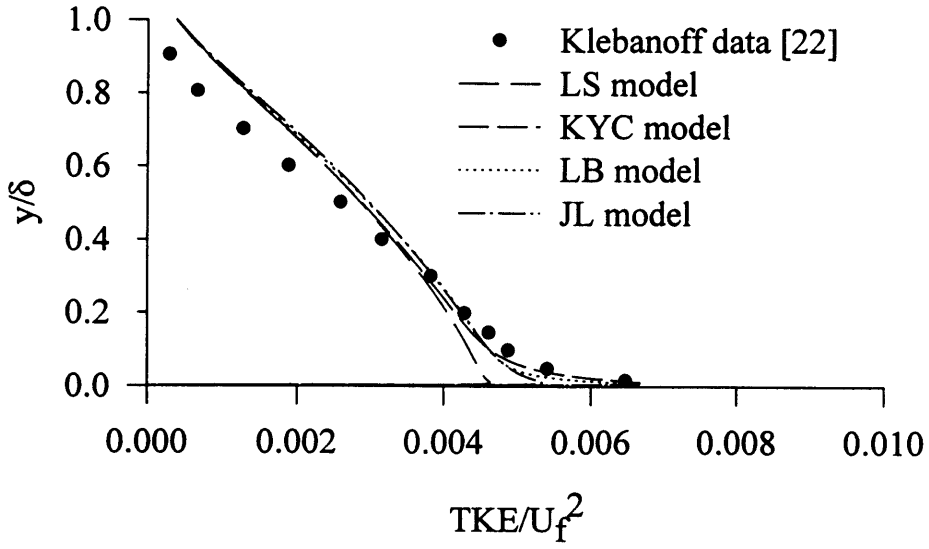

Fig. 1c. TKE profiles for baseline case ($Tu_i = 1\%$).

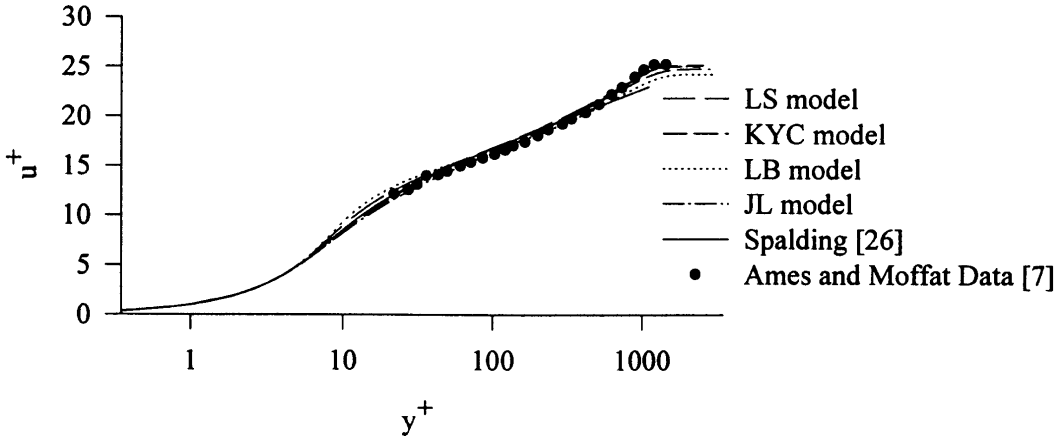

Fig. 1d. Velocity profiles for baseline case ($Tu_i = 1\%$).

number given by equation (13). As expected the results for skin friction coefficient and velocity and TKE profiles did not change at all. Stanton number results (Fig. 1e) improved in comparison to the constant Pr_t case. All the models except the LB model predicted within $\pm 4\%$ of the data and equation (19) whereas the LB model over predicted by about 10% in comparison to empirical data and equation (19). A plausible reason for the LB model not predicting as well as the other models for skin friction and heat transfer coefficients might be due to the fact that predictions using this model are somewhat sensitive to the constants in the equations for f_1 and f_μ as reported by the authors Lam and Bremhorst [27].

Thus, insofar as baseline cases are concerned, it can be said that all these models are good. With this in mind, the focus will be shifted to the primary aspect of this study, that is, the performance of all these models under high FST ($Tu_i > 5\%$) conditions. There is no definite physical reason as to why $Tu_i > 5\%$ is chosen as high FST. This value of 5% or higher is chosen for the purpose of definition in this paper to represent high FST. Two data sets, one of Blair [6, 32] (initial turbulence intensity, $Tu_i = 6.53\%$ calculated according to equation (2)) and the other of Ames and Moffat [7] (initial turbulence intensity, $Tu_i = 25.7\%$ calculated according to equation (2)) were chosen to be compared against the predictions. In order to enable clear distinction of the two data sets, the data set of Blair will be referred to as the one with

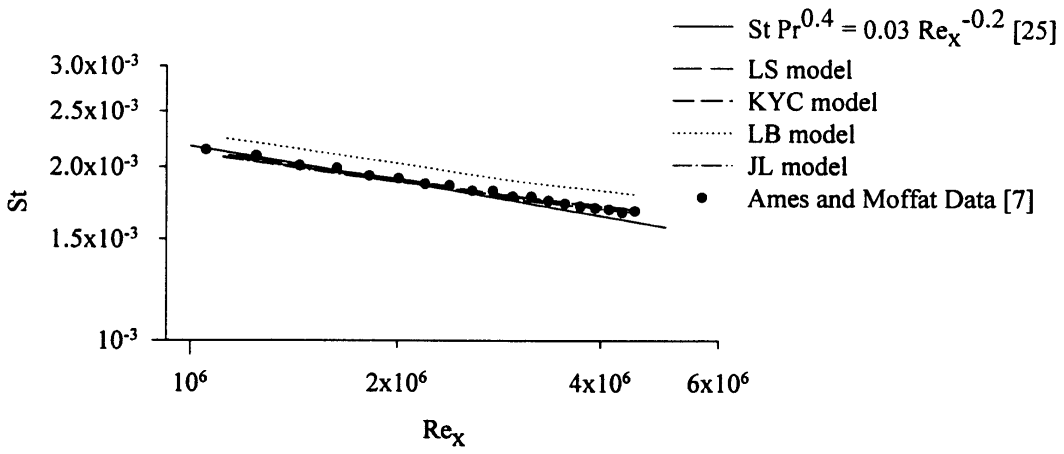

Fig. 1e. Stanton number for baseline case ($Tu_i = 1\%$, variable Pr_t).

moderately high FST and that of Ames and Moffat will be referred to as the one with very high FST.

4.2. Model predictions in the turbulent region for moderately high FST ($\mathrm{Tu}_i = 6.53\%$)

This data was obtained in the United Technologies Research Center (UTRC) boundary layer wind tunnel. This tunnel was designed to generate large scale two-dimensional, incompressible boundary layers with Reynolds numbers and FST levels typical in turbomachinery environments. High FST was generated by inserting various square array biplane grids constructed from rectangular bars at the entrance to the main tunnel contraction. The boundary layer test surface consisted of a flat plate subjected to uniform heat flux. Uncertainties in measurements were $\pm 2/5\%$ for St, $\pm 1.5\%$ for integral thicknesses, $\pm 1\%$ for location Reynolds numbers and $\pm 3\%$ for $c_f/2$.

All the calculations were started at $x = 0.318$ m with a virtual origin which was adjusted to match Re_θ at $x = 0.318$ m with measurements. The free stream velocity was 30.48 m s^{-1}. Providing a correct initial value of turbulent dissipation rate in the free stream ($\tilde{\varepsilon}_\infty$) is necessary for a valid evaluation of all models [14]. This initial value was obtained from the free stream forms of k-ε equations given by equations (15) and (16) and experimental data. Equations (15) and (16) combine to give the following equation:

$$\frac{\mathrm{d}^2 k_\infty}{\mathrm{d}x^2} - \frac{c_2 f_2}{k_\infty}\left(\frac{\mathrm{d}k_\infty}{\mathrm{d}x}\right)^2 = 0 \tag{21}$$

This equation was solved using the Runge–Kutta scheme [31] using experimental values of k_∞ at beginning and end of calculations. Once $\mathrm{d}k_\infty/\mathrm{d}x$ was obtained, $\tilde{\varepsilon}_\infty$ was calculated using equation (15). Figure 2a shows the decay of TKE as calculated by TEXSTAN (the LS model is shown as an example) compared with the experimental decay. The prediction was obtained by using $\tilde{\varepsilon}_\infty$ calculated by the method just mentioned. It is very clear from the figure that TKE decay so calculated, matches very well with the experimental information. ε_f in the figure is the initial free stream turbulent dissipation rate and is nothing but the initial value of $\tilde{\varepsilon}_\infty$.

Figure 2b shows the plot of friction coefficient, where the predictions of all the four models are compared with Blair's data. The data clearly shows that there is definite increase in friction coefficient (maximum of about 11%) when compared to the standard correlation, equation (18). All the models except LB over predict within 9% of the data whereas the LB model over predicts within 13%. It is to be noted that predictions are better at higher Re_θ indicating calculation of incorrect slope by the models. Stanton number versus Re_x is shown in Fig. 2c. The increase in St compared to the standard correlation, equation (19), is about 14%. The LS, JL and KYC models over predict by a maximum of about 10% and the LB model over predicts within 16% when compared to the best fit line ($St = 0.0017 + 741.61/Re_x$) which was drawn as a result of the scatter in data. Again predictions of the slope are wrong. TKE profiles (at $x = 1.73$ m from the leading edge) in Fig. 2d show clearly that all models under-predict (up to about 28%) in the boundary layer. As in the baseline case, here again, the JL and LS models have problems predicting the peak value. Plots for displacement and momentum thicknesses are shown in Figs 2e and f respectively. It is evident that the predictions of all the models agree very well with the data. These models were again tested for Pr_t given by equation (13). The results of skin friction coefficient and TKE profiles did

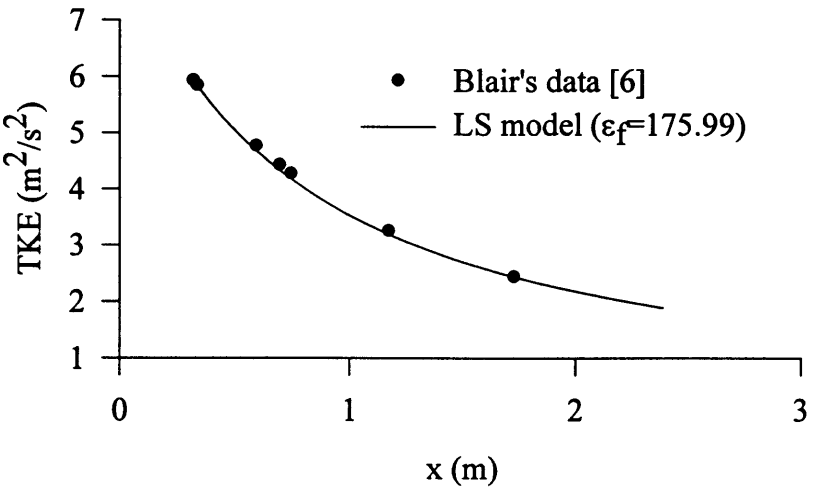

Fig. 2a. TKE decay for moderately high FST (Tu_i = 6.53%).

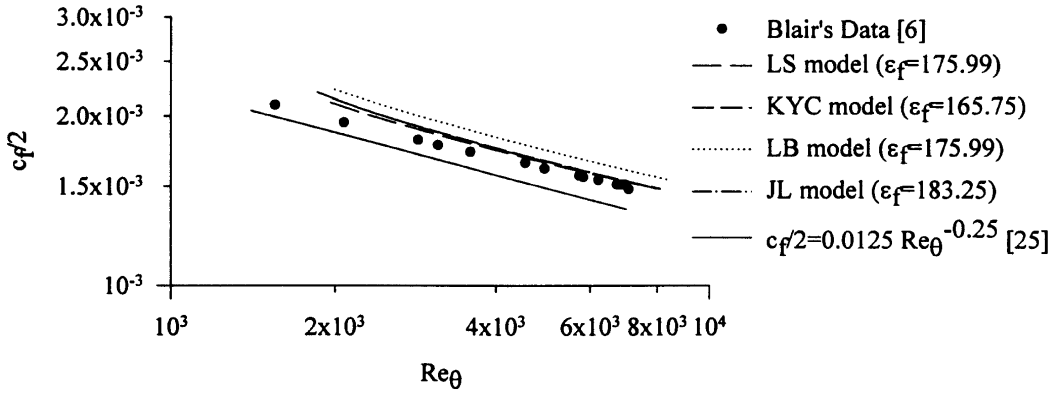

Fig. 2b. Skin friction coefficient for moderately high FST (Tu_i = 6.53%).

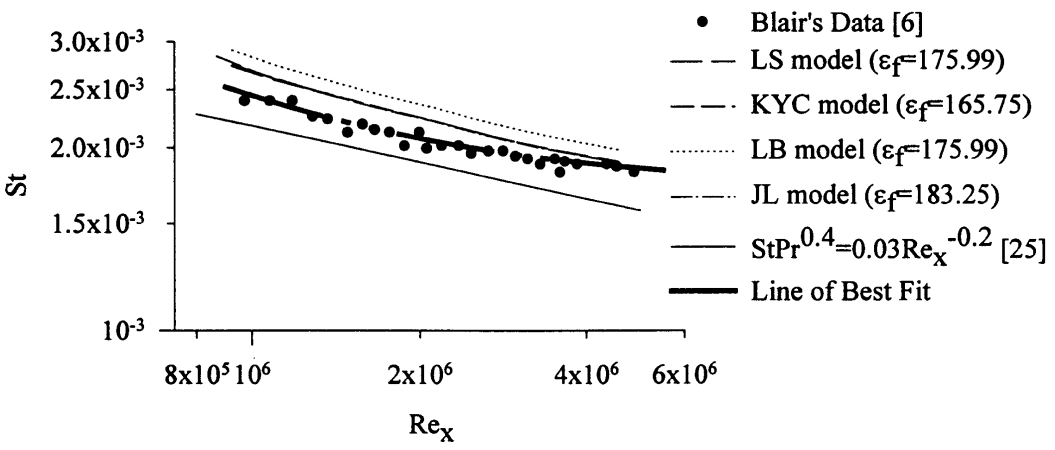

Fig. 2c. Stanton number for moderately high FST (Tu_i = 6.53%).

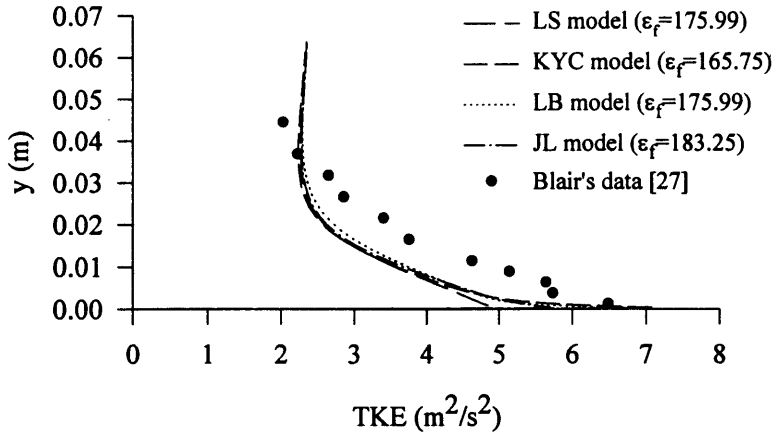

Fig. 2d. TKE profiles for moderately high FST (Tu_i = 6.53%, x = 1.73 m).

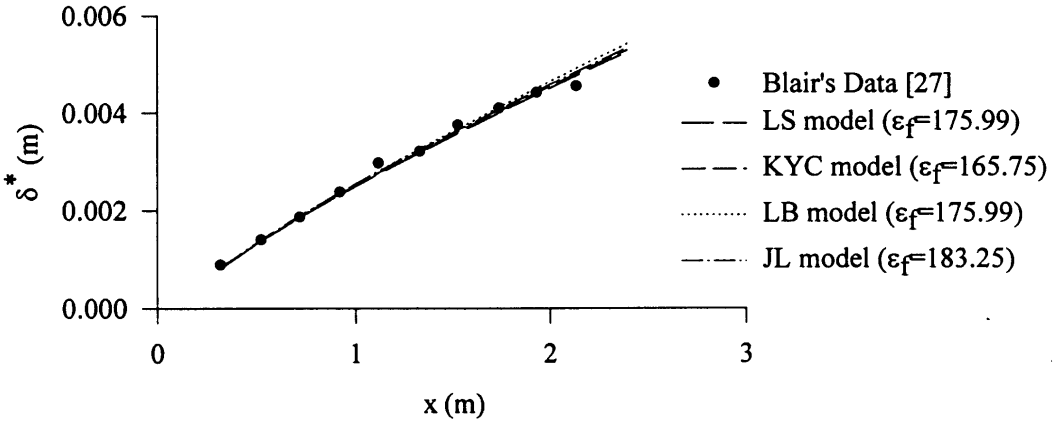

Fig. 2e. Displacement thickness for moderately high FST (Tu_i = 6.53%).

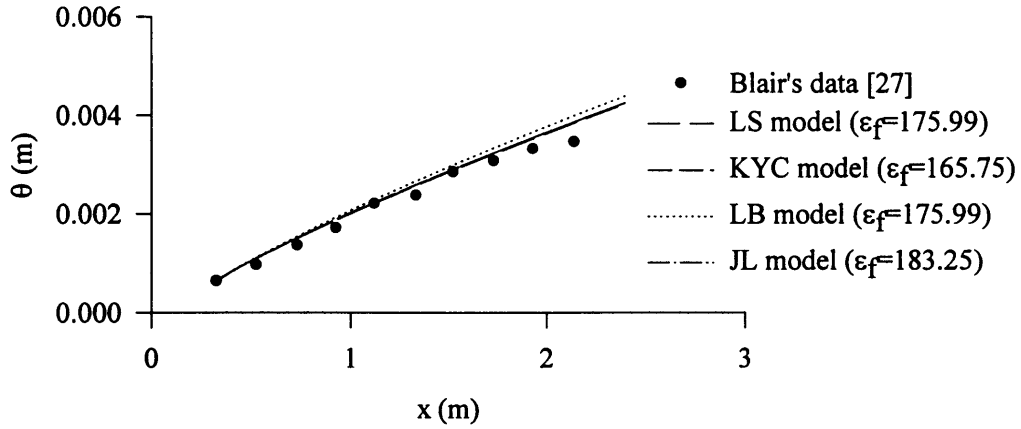

Fig. 2f. Momentum thickness for moderately high FST (Tu_i = 6.53%).

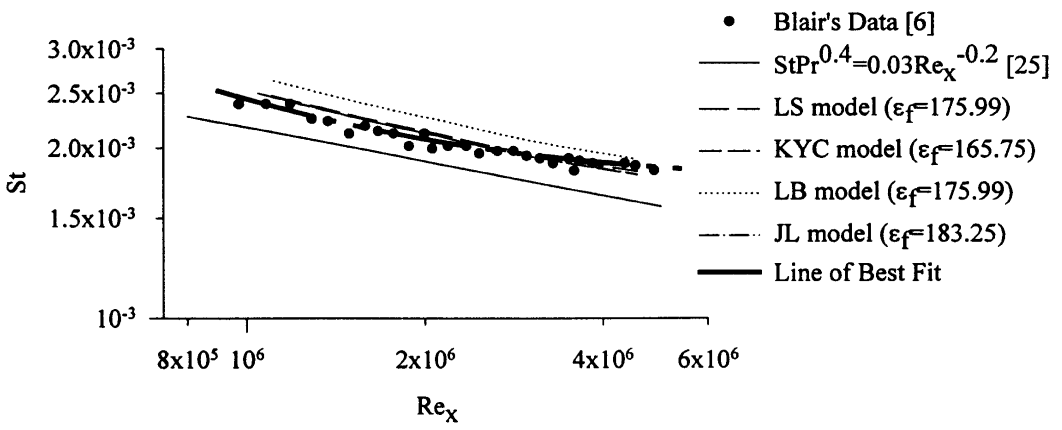

Fig. 2g. Stanton number for moderately high FST ($Tu_i = 6.53\%$, variable Pr_t).

not change, but Stanton number did change like in the baseline case (Fig. 2g). The figure clearly indicates a marked improvement in the predictions. All models barring the LB model predict within $\pm 4\%$ of the best fit line. The LB model over predicts within 11% of the best fit line.

4.3. Model predictions in the turbulent region for very high FST ($Tu_i = 25.7\%$)

This data was obtained in a closed loop wind tunnel. Like Blair's experimental facility, a guarded constant heat flux surface was designed specifically for this study. The turbulence generator used for this research endeavour was designed to produce a flow similar to the exit flow of a modern annular combustor. Due to lack of detailed hydrodynamic data, the data of Yavuzkurt and Batchelder [10] was referred to for the same. This data was also taken from experiments conducted by the authors in the same facility for similar FST under identical conditions. Again, uncertainties in measurements were $\pm 6\%$ for TKE, $\pm 4.5\%$ for $c_f/2$, $\pm 4\%$ for St, and about $\pm 10\%$ for integral thicknesses and length scales. All the calculations were started at $x = 0.157$ m with a virtual origin which was adjusted to match Re_θ at $x = 0.157$ m with measurements. The free stream velocity was 6 m s^{-1}. As shown in Fig. 3a, the friction coefficient increases by about 15% when compared to Kays and Crawford correlation [30]. Again, all models over predict by at least 35% and go up to more than 100%. The slopes of the predictions do not match the slope of the data. The KYC model predicts the worst. Stanton number results (shown in Fig. 3b) indicate the same trend as skin friction coefficient. The increase in St is about 18% when compared to the Kays and Crawford correlation [30]. All models over predict again and this can go up as high as 80% and slopes are also incorrect. The predictions seemingly appear to improve at higher Reynolds numbers, but the wrong slopes are the cause of that. It is apparent from TKE profiles (at $x = 2.08$ m from the leading edge) in Fig. 3c that boundary layer growth is unrealistic. Similar to the case of Blair's data TKE is under predicted ($>15\%$) across the boundary layer by all the models. Of course, near the wall, TKE is under predicted much more. Unlike Blair's data though, all models have problems predicting the peak value of TKE (0.5795 m^2 s^{-2}). The plots for displacement and momentum and thickness represented by Figs 3d and e respectively indicate that all the models over predict by as much as 100% if not more. It is speculated that this might be due to unrealistic mixing [18]. Figure 3f shows the plot of Stanton number for Pr_t calculated by equation (13). Results improve in comparison to the constant Pr_t case, but the slopes are still incorrect and predictions are still far from being reasonable.

5. Conclusions and future work

The results from the foregoing sections clearly indicate that predictions become poorer (up to more than 50% for skin friction coefficient, Stanton number and TKE) as FST increases. For the moderately high FST case, Stanton number and skin friction coefficient results are still within acceptable limits (within 13% of the data) for all the models. TKE results are not within reasonable limits (under prediction up to 28%), and here again, the deficiency of the JL and LS models in predicting the peak values is obvious. The JL model predicts a peak value of 4.94 and the LS model predicts a peak value of 5.70, whereas the peak value of the data is 6.50. For the very high FST case, it can be unambiguously stated that all the results are not within acceptable limits.

As FST increases, diffusion of high Tu fluid into the boundary layer should increase, thereby increasing levels of TKE within the boundary layer. It is speculated at this

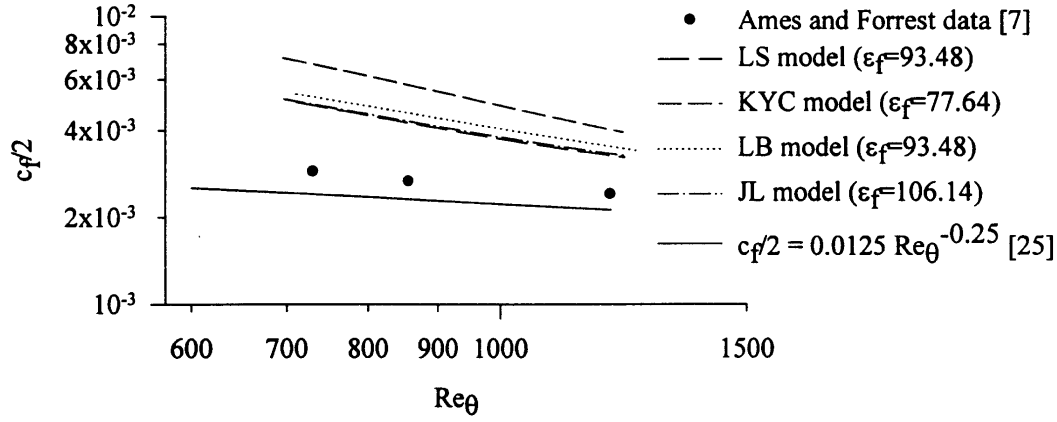

Fig. 3a. Skin friction coefficient for very high FST (Tu_i = 25.7%).

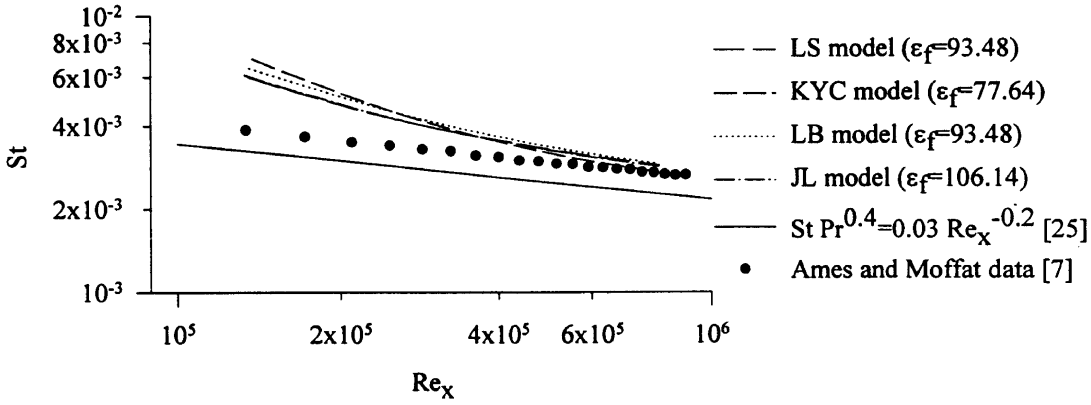

Fig. 3b. Stanton number for very high FST (Tu_i = 25.7%).

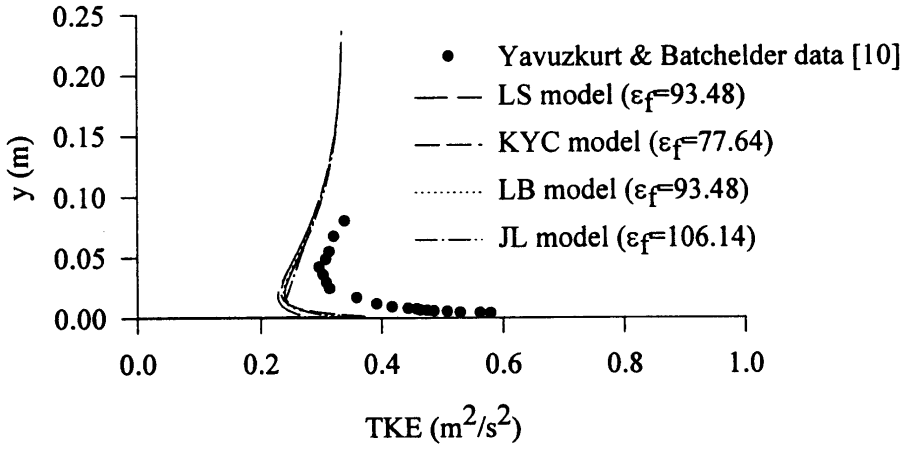

Fig. 3c. TKE profiles for very high FST (Tu_i = 25.7%, x = 2.08 m).

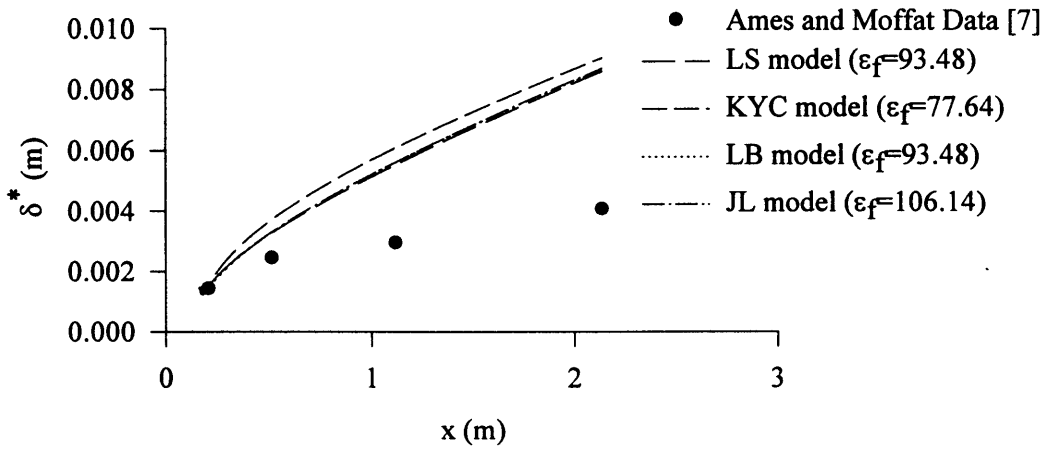

Fig. 3d. Displacement thickness for very high FST (Tu_i = 25.7%).

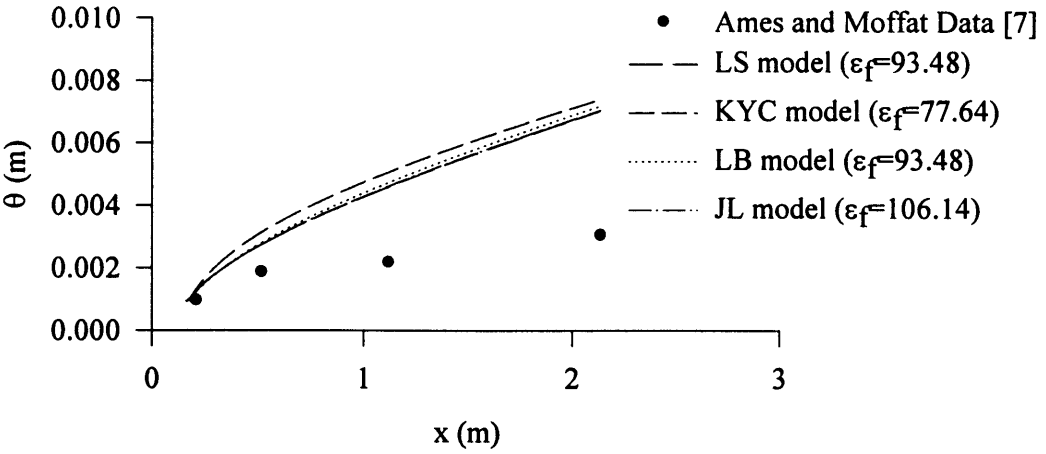

Fig. 3e. Momentum thickness for very high FST (Tu_i = 25.7%).

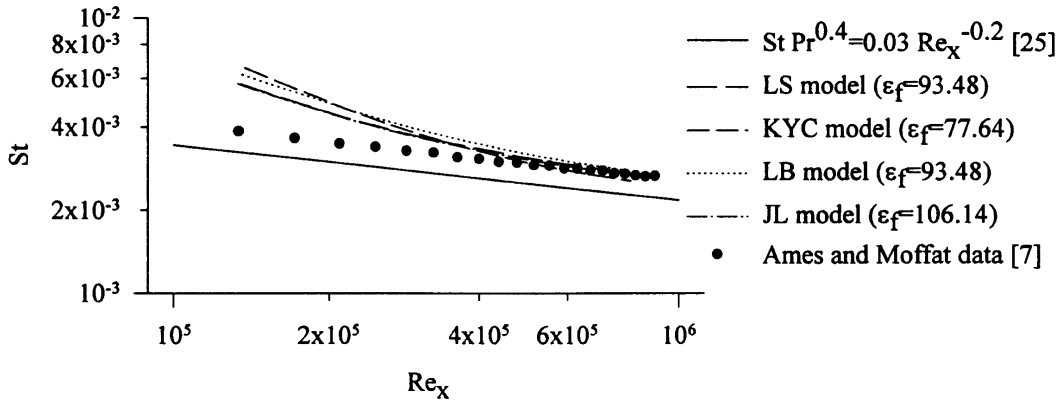

Fig. 3f. Stanton number for very high FST (Tu_i = 25.7%, variable Pr_t).

juncture that the failure of TKE prediction at high FST levels might be caused by the models not being able to predict the phenomena of added diffusion or increased levels of TKE. Improving TKE predictions should also improve predictions of Stanton number and skin friction coefficient. A direction to follow for improving the above predictions would be to examine carefully the TKE equation and modify it to enhance the levels of TKE in the boundary layer. Future work will focus on modifying the k–ε model for improving TKE predictions and thereby improving all hydrodynamic and heat transfer predictions.

Appendix

Initial profile of k

The TKE profile is computed in the near-wall region by computing the turbulent viscosity using mixing length, and then equating it to the Hasid–Poreh [33] one-equation model for turbulent viscosity assuming that the length scale is κy. This requires iteration because the one-equation model uses Reynolds number based on TKE (Re_k) in its damping function.

$$l = \kappa y, \quad f_\mu = 1 - \exp(-0.00115 y^+)$$

$$k_{\text{old}} = \left\{ \frac{\nu_t}{\nu} \left(\frac{\nu}{2.45 l f_\mu (1 - \exp[-y^+/A^+])} \right) \right\}^2 \tag{A1}$$

where

$$\frac{\nu_t}{\nu} = \kappa^2 y^{+^2} \left[1 - \exp\left(-\frac{y^+}{A^+} \right) \right]^2 \frac{\partial u^+}{\partial y^+}$$

and $u^+ = U/u^*$, $y^+ = y u^*/\nu$ and $u^* = \sqrt{\tau_w/\rho}$

$\kappa = 0.41$ and $A^+ = 25$

$$Re_k = \frac{k_{\text{old}}^{0.5} l}{\nu} \quad \text{and} \, f_\mu = 1 - \exp(-0.029 Re_k) \tag{A2}$$

$$k_{\text{new}} = \left[\frac{\nu_t}{\nu} \frac{\nu}{0.548 f_\mu l} \right]^2 \tag{A3}$$

If $\dfrac{|k_{\text{new}} - k_{\text{old}}|}{k_{\text{old}}} \leqslant 0.01$, then $k = k_{\text{new}}$

otherwise, $k_{\text{old}} = \dfrac{k_{\text{new}} + k_{\text{old}}}{2}$ and iterate

In equations (A1)–(A3), l is the mixing length, k_{old} is the TKE calculated by computing the turbulent viscosity using mixing length and k_{new} is the TKE using the Hasid–Poreh [33] one-equation model for turbulent viscosity. The free stream value of TKE is calculated as follows:

$$k_\infty = \frac{3}{2} (T u U_\infty)^2 \quad \text{where} \quad Tu = \left(\frac{\sqrt{\overline{u'^2}}}{U} \right)_\infty . \tag{A4}$$

For the outer region, the TKE profile is curve fit between the last inner region value and its free stream value using a third order polynomial.

Initial profile of ε

In the inner region, the dissipation rate is computed using the equation,

$$\tilde{\varepsilon} = \frac{0.164 k^{1.4}}{\ell} \tag{A5}$$

and the free stream value is calculated using

$$\tilde{\varepsilon}_\infty = \frac{0.09 k_\infty^{1.5}}{0.3\delta} . \tag{A6}$$

Again, in the outer region, the $\tilde{\varepsilon}$ profile is calculated in the same manner as the TKE profile.

Acknowledgement

The authors would like to express their gratitude to Professor M. E. Crawford at the University of Texas at Austin for his helpful discussions about TEXSTAN.

References

[1] P. Koutmos, J.J. McGuirk, Isothermal flow in a gas turbine combustor, Experiments in Fluids 7 (1989) 344–354.
[2] J.C. Simonich, P. Bradshaw, Effect of free-stream turbulence on heat-transfer through a turbulent boundary layer, ASME Journal of Heat Transfer 100 (1978) 671–677.
[3] A.A. Pedisius, P.-V.A. Kazimekas, A.A. Slanciauskas, Heat transfer from a plate to a high-turbulence air flow, Heat Transfer-Soviet Research 11 (1979) 125–133.
[4] P.E. Hancock, P. Bradshaw, The effect of free-stream turbulence on turbulent boundary layers, ASME Journal of Fluids Engineering 105 (1983) 284–289.
[5] S. Yavuzkurt, Effects of free-stream turbulence on the instantaneous heat transfer in a wall jet flow, ASME Journal of Turbomachinery 119 (1997) 359–362. Engineering (1975) 234–241.
[6] M.F. Blair, M.J. Werle, The influence of free-stream turbulence on zero pressure gradient fully turbulent boundary layer. UTRC report, R80-914388-12. UTRC, East Hartford, 1980.
[7] F.E. Ames, Heat transfer with high intensity, large scale turbulence: The flat plate turbulent boundary layer and the cylindrical stagnation point. Report HMT-44. Department of Mechanical Engineering, Stanford University, 1990.
[8] R. MacMullin, W. Elrod, R. Rivir, Free-stream turbulence from a circular wall jet on a flat plate heat transfer and boundary layer flow, ASME Journal of Turbomachinery 111 (1989) 78–86.
[9] P.K. Maciejewski, R.J. Moffat, Heat transfer with very high free-stream turbulence: Part I—experimental data, ASME Journal of Heat Transfer 114 (1992a) 827–833.

[10] S. Yavuzkurt, K. Batchelder, A correlation for heat transfer under high free stream turbulence conditions. Proceedings of the Ninth Symposium on Turbulent Shear Flows. Kyoto, Japan, 1993, P104-1–P10404.
[11] K.A. Thole, D.G. Bogard, High freestream turbulence effects on turbulent boundary layers, ASME Journal of Fluids Engineering 118 (1996) 276–284.
[12] S.P. Harasgama, F.H. Tarada, R. Baumann, M.E. Crawford, S. Neelakantan, Calculation of heat transfer to turbine blading using two-dimensional boundary layer methods. ASME Paper No: 93-GT-79.
[13] R.C. Schmidt, S.V. Patankar, Prediction of transition on a flat plate under the influence of free-stream turbulence using low-Reynolds-number two-equation turbulence models. ASME Paper 87-HT-32, 1987, pp. 1–9.
[14] K. Sieger, A. Schulz, M.E. Crawford, S. Wittig, An evaluation of low-Reynolds number k, ε-turbulence models for predicting transition under the influence of free-stream turbulence and pressure gradient. Proceedings of Second International Symposium on Engineering Modelling and Measurements. Florence, Italy, 1993, p. 1–10.
[15] M.F. Blair, M.J. Werle, Combined influence of free-stream turbulence and favorable pressure gradients on boundary layer transition and heat transfer. UTRC Report R81-914388-17, 1981.
[16] K. Rud, S. Wittig, Laminar and transitional boundary layer structures in accelerating flow with heat transfer, ASME Journal of Turbomachinery 108 (1986) 116–123.
[17] A.M. Savill, Predicting transition induced by free-stream turbulence. IAHR/ERCOFTAC Turbulence Modelling SIG Seminar, Delft, 1992.
[18] O. Kwon, F.E. Ames, Advanced k–epsilon modelling of heat transfer. NASA contractor report, 4679, Allison Engine Company, Indianapolis, 1995.
[19] P.A. Durbin, Application of a near-wall turbulence model to boundary layers and heat transfer, International Journal of Heat and Fluid Flow 14 (1993) 316–323.
[20] E. Fridman, Simulation of heat transfer from flow with high free-stream turbulence to turbine blades, ASME Journal of Trubomachinery 119 (1997) 284–291.
[21] R.J. Volino, A new model for free-stream turbulence effects on boundary layers. ASME Paper 97-GT-122, 1997, pp. 1–9.
[22] W. Rodi, G. Scheuerer, Calculation of turbulent boundary layers under the effect of free stream turbulence. Proceedings of the Fifth Symposium on Turbulent Shear Flows, Cornell University, 1985, pp. 2.19–2.25.
[23] W. Rodi, G. Scheuerer, Calculation of heat transfer to convection-cooled gas turbine blades, ASME Journal of Engineering for Gas Turbines and Power 107 (1985) 620–627.
[24] W.P. Jones, B.E. Launder, The prediction of laminarization with a two equation model of turbulence, International Journal of Heat and Mass Transfer 15 (1972) 301–314.
[25] B.E. Launder, B.I. Sharma, Application of the energy-dissipation model of turbulence to the calculation of flow near a spinning disc, Letters in Heat and Mass Transfer 1 (1974) 131–138.
[26] C.K.G. Lam, K.A. Bremhorst, A modified form of the k–ε model for predicting wall turbulence, ASME Journal of Fluids Engineering 103 (1991) 456–460.
[27] K.Y. Chien, Predictions of channel and boundary-layer flows with a low-Reynolds-number turbulence model, AIAA Journal 20 (1982) 33–38.
[28] M.E. Crawford, Simulation codes for calculation of heat transfer to convectively cooled turbine blades, VKI-LS-1986-06, Convective Transfer and Film Cooling in Turbomachinery, 1986.
[29] S.V. Patankar, Heat and Mass Transfer in Boundary Layers, Morgan-Grampian Books Ltd., London, 1967, p. 138.
[30] W.M. Kays, M.E. Crawford, Convective Heat and Mass Transfer, 3rd ed., McGraw-Hill Book Company, New York, 1993, p. 601.
[31] F.M. White, Viscous Fluid Flow, 2nd ed., McGraw-Hill Book Company, New York, 1991, p. 614.
[32] M.F. Blair, D.E. Edwards, The effects of free-stream turbulence on the turbulence structure and heat transfer in zero pressure gradient boundary layers. UTRC report, R82-915634-2. UTRC, East Hartford, 1982.
[33] S. Hasid, M. Poreh, A turbulent energy model for flows with drag reduction, Journal of Fluids Engineering (1975) 234–241.